iScience

CellPress
OPEN ACCESS

Article

Scaffold-induced compression enhances ligamentization potential of decellularized tendon graft reseeded with ACL-derived cells

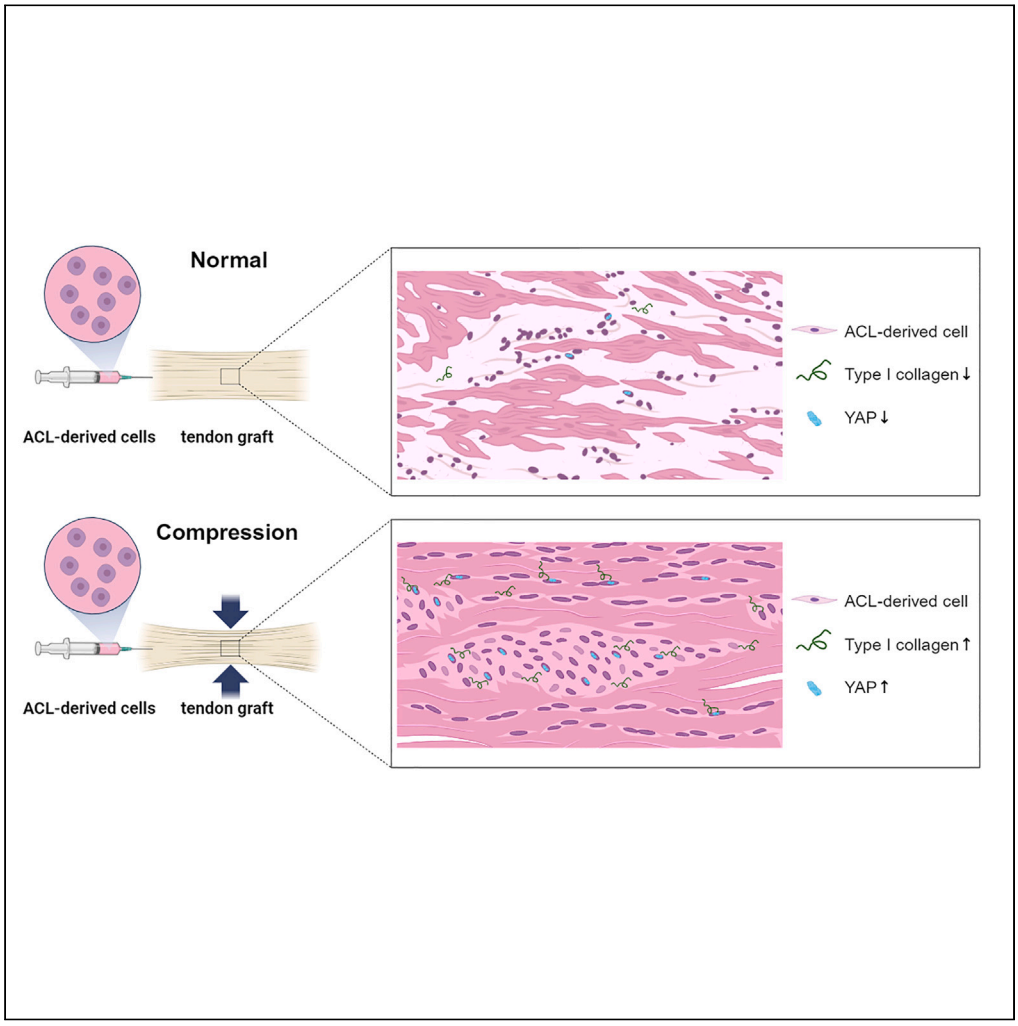

Jinsung Park, Hyunsoo Soh, Sungsin Jo, ..., Tae-Hwan Kim, Il-Hoon Sung, Jin Kyu Lee

jklee77@hanyang.ac.kr

Highlights

Compressive stimulation given to the graft increases cell integration and survival

ACL-derived cells in the compressed graft enhance the expression of type I collagen

Type I collagen expression correlates with the translocation of YAP into the nucleus

Park et al., iScience 26, 108521
December 15, 2023
https://doi.org/10.1016/j.isci.2023.108521

iScience

CellPress
OPEN ACCESS

Article

Scaffold-induced compression enhances ligamentization potential of decellularized tendon graft reseeded with ACL-derived cells

Jinsung Park,[1,5] Hyunsoo Soh,[2,5] Sungsin Jo,[1] Subin Weon,[1] Seung Hoon Lee,[1] Jeong-Ah Park,[1] Myung-Kyu Lee,[3] Tae-Hwan Kim,[1,4] Il-Hoon Sung,[2] and Jin Kyu Lee[1,2,6,*]

SUMMARY

Anterior cruciate ligament (ACL) reconstruction is often performed using a tendon graft. However, the predominant synthesis of fibrotic scar tissue (type III collagen) occurs during the healing process of the tendon graft, resulting in a significantly lower mechanical strength than that of normal ACL tissue. In this study, ACL-derived cells were reseeded to the tendon graft, and scaffold-induced compression was applied to test whether the compressive force results in superior cell survival and integration.

Given nanofiber polycaprolactone (PCL) scaffold-induced compression, ACL-derived cells reseeded to a tendon graft demonstrated superior cell survival and integration and resulted in higher gene expression levels of type I collagen compared to non-compressed cell-allograft composites *in vitro*. Translocation of Yes-associated protein (YAP) into the nucleus was correlated with higher expression of type I collagen in the compression group. These data support the hypothesis of a potential role of mechanotransduction in the ligamentization process.

INTRODUCTION

Anterior cruciate ligament reconstruction (ACLR) is one of the most frequently performed surgical procedures in orthopedic sports medicine.[1–4] ACLR using a tendon graft is the current gold standard of care to treat complete ACL rupture.[5] Both tendons and ligaments are similarly composed of dense extracellular matrix (ECM), mainly containing type I collagen and proteoglycans. However, their microstructural composition and arrangement differ to provide the different mechanical properties required.[6] For successful healing following ACLR, the implanted tendon graft requires biological remodeling and maturation toward a ligament-like structure, often referred to as the ligamentization process.[7,8] Several *in vivo* studies have shown that the ligamentization process involves cellular invasion consisting of fibroblasts integrating into the ECM of the tendon graft in the early stage. The remodeling process of the tendon graft continues beyond one year to achieve biological and mechanical properties similar to those of native ACL.[9–12] However, the predominant synthesis of type III collagen during the remodeling process eventually leads to scar tissue formation, resulting in a significantly lower mechanical strength than that of normal ACL tissue.[13,14] Several studies have found increased quantification and expression of type III collagen markers in the healing graft, even after long-term healing of up to 2 years.[15–17] Various tissue engineering strategies have been introduced to improve the healing of the tendon graft in ACLR surgery.[18–20] Our group has previously demonstrated that ACL-derived cells, when reseeded to the tendon graft, show an earlier ability to survive and integrate into tendon ECM, resulting in a higher gene expression level of type I collagen compared to that in adipose tissue-derived mesenchymal stem cells (MSCs).[21]

Alterations in the mechanical environment could result in changes in the expression of cytokines, transcription factors, and ECM proteins that can eventually alter the biological and structural nature of the tendon.[22–24] Indeed, excessive mechanical load with ACLR leads to accumulation of macrophages, which is detrimental to the remodeling and healing of the tendon graft. However, controlled mechanical loading can be beneficial, eventually leading to increased tendon-specific gene expression and enhancing tendon graft healing.[25] Several studies reported positive effects of compressive load application on matrix remodeling and fibrocartilage formation on tendon grafts[22–24]; however, behaviors of reseeded cells within the ECM of tendon grafts to mechanical loadings have not been studied. The stiffness of ECM is a universal mechanical cue that regulates cell behavior.[26] The Yes-associated protein (YAP) is the main transcription factor that plays a central role in the delivery of such mechanical cues from surrounding cells to the transcriptional machinery of the nucleus. This induces the expression of

[1]Hanyang University Institute for Rheumatology Research, Seoul, Republic of Korea
[2]Department of Orthopaedic Surgery, Hanyang University Hospital, Seoul, Republic of Korea
[3]Department of Research and Development, Korea Public Tissue Bank, Seongnam-si, Gyeonggi-do, Korea
[4]Department of Rheumatology, Hanyang University Hospital for Rheumatic Disease, Seoul, Republic of Korea
[5]These authors contributed equally
[6]Lead contact
*Correspondence: jklee77@hanyang.ac.kr
https://doi.org/10.1016/j.isci.2023.108521

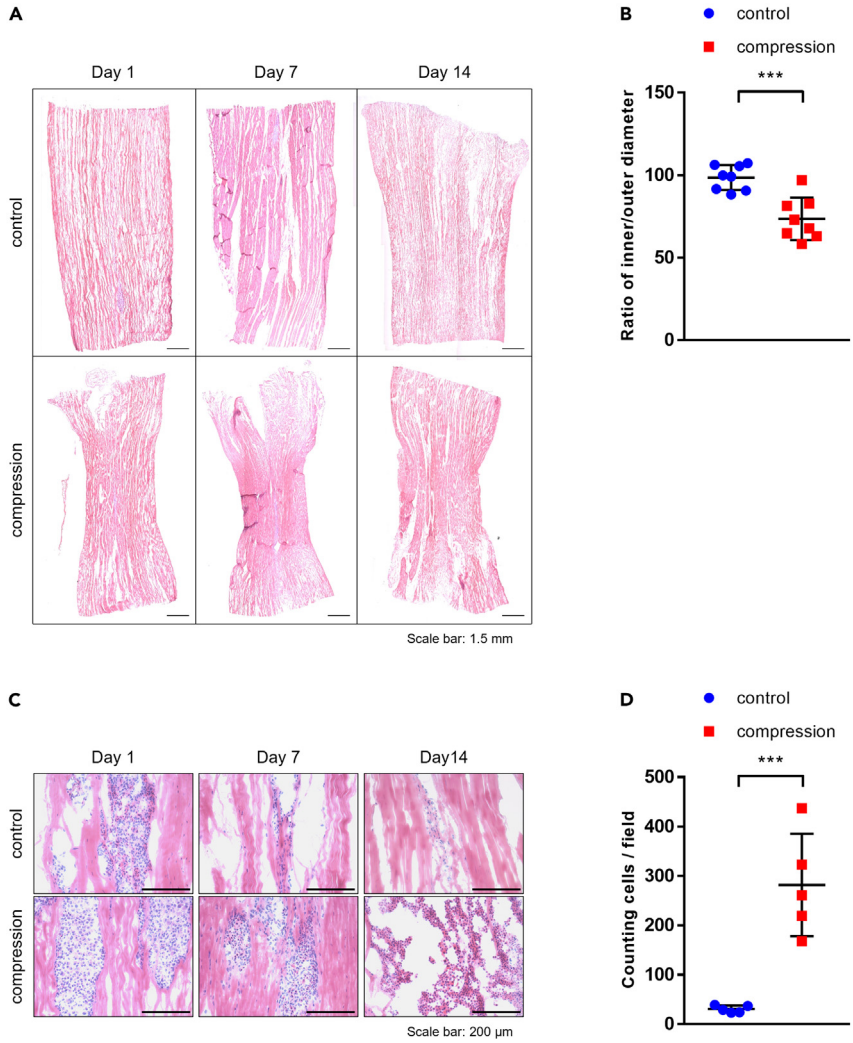

Figure 1. Graft compression ratio, cell integration, and survival

(A) Entire specimens were stained with H&E.

(B) Compressive ratio of each tendon allograft was measured with ImageJ (n = 8).

(C) Cell integration was analyzed by H&E staining. Magnification ×100, scale bar: 200 μm.

(D) The number of ACL-derived cells in both groups was counted on five consecutive slides on day 14 (n = 5). *, $p < 0.05$; **, $p < 0.01$; ***, $p < 0.001$; ns: not significant. Statistical analysis of the data was performed using a two-tailed paired t test. Data are shown as the mean ± SEM.

cell-proliferative and anti-apoptotic genes.[27–30] Furthermore, recent studies reported that the YAP upregulates type I collagen expression in various cell types, including human scleral fibroblasts, human bone marrow MSCs, and human nucleus pulposus cells, which is crucial for the success of ligamentization of the tendon graft[31–33]

Hence, based on the occurrence of scaffold-induced compression, we tested the hypothesis that ACL-derived cells reseeded to the tendon graft would demonstrate superior cell survival and integration. We also hypothesized that this would result in higher gene expression levels of YAP and ligament-related proteins (e.g., type I collagen) compared to non-compressed cell-allograft composites *in vitro*.

RESULTS

Graft compression ratio, cell integration, and survival

Representative cryo-sectioned slides showing the whole length of the graft were selected for measurements of the ratio of inner/outer diameter (Figure 1A). The ratio of inner/outer diameter (diameter at the middle divided by the mean of the diameters at the two ends) was 73.51% ± 4.534% (n = 8) for the graft with scaffold-induced compression (compression group) and 98.54% ± 2.68% (n = 8) for the non-compression group (Figure 1B) ($p < 0.001$). Histologic features observed from H&E-stained slides showed a different pattern of cell

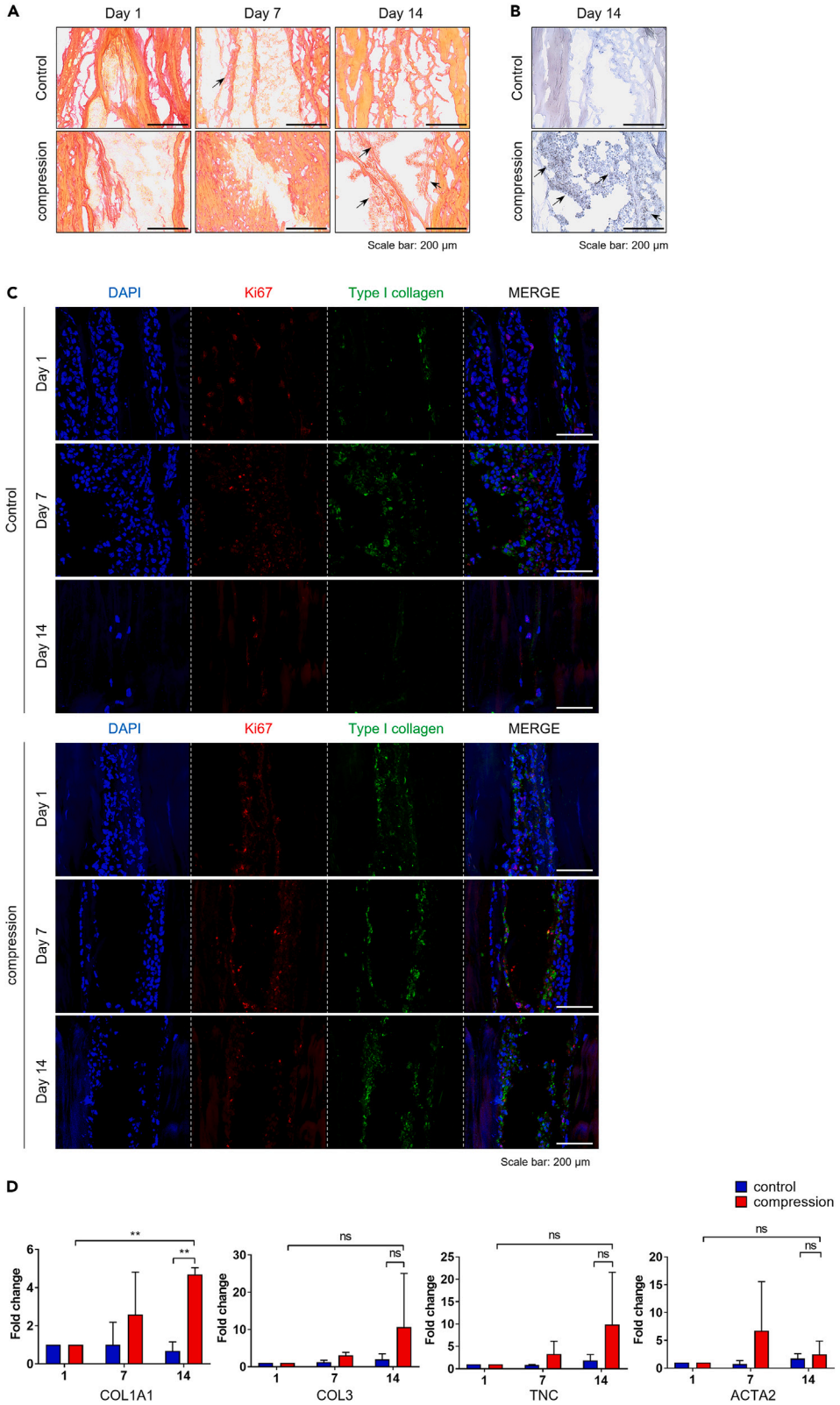
A
Day 1
Day 7
Day 14
Control
compression
Scale bar: 200 μm
B
Day 14
Control
compression
Scale bar: 200 μm
C
DAPI
Ki67
Type I collagen
MERGE
Control
Day 1
Day 7
Day 14
compression
Day 1
Day 7
Day 14
Scale bar: 200 μm
D
control
compression
Fold change
COL1A1
COL3
TNC
ACTA2
ns
**

Figure 2. Matrix protein contents and gene expression

(A) ACL-derived injected cellular tendon allograft was stained with Picrosirius red for types I and III collagen. Magnification ×100, scale bar: 200 μm.

(B) IHC was stained for type I collagen on day 14. Magnification ×200, scale bar: 100 μm.

(C) Co-immunofluorescence staining was performed on days one, seven, and 14 for Ki67 (red) and type I collagen (green).

(D) The mRNA expression level of ligament-related markers (COL1A1, COL3, and tenascin C) and smooth muscle actin (ACTA2) was analyzed by RT-qPCR (n = 3). *, $p < 0.05$; **, $p < 0.01$; ***, $p < 0.001$; ns: not significant. Statistical analysis of the data was performed using a two-way ANOVA. Data are shown as the mean ± SEM.

integration and survival between compressed and non-compressed cell-graft composites. On day 1, a cluster of injected cells was evident along the graft's intra-fascicular openings, indicating successful injections of cells. In the compression group, a large number of cells integrated into the matrix on day seven and day 14; however, in the non-compression group, although a proportion of cells showed integration into the matrix on day seven, only a small number of cells that integrated into the matrix were found on day 14 (Figure 1C). The number of cells that integrated was counted on day 14. A significantly higher number of cells was found in the compression group; only a limited number of cells was found in the non-compression group (Figure 1D) ($p < 0.001$).

Matrix protein contents and gene expression

Immunohistochemical (IHC) staining showed more consistent collagen staining in the cell-graft composites of the compression group compared to the non-compression group on days seven and 14 (Figures 2A and 2B). Immunofluorescence (IF) staining for Ki-67 and type I collagen demonstrated more pronounced expression of type I collagen in Ki-67 positive ACL-derived cells in the compression group compared to the non-compression group on day 14 (Figure 2C). An mRNA expression level analysis confirmed significantly higher expression of type I collagen on day 14 in the compression group compared to the non-compression group ($p < 0.01$). However, other ligament-related markers, including tenascin C and smooth muscle A, showed no significant difference between the two groups (Figure 2D).

Expression of YAP

IHC staining showed more potent staining for YAP (Figure 3A) and significantly higher gene expression levels of YAP in the compression group compared to the non-compression group on day 14 (Figure 3B) ($p < 0.001$). IF staining on day 14 confirmed YAP translocation into the nucleus of ACL-derived cells in the compression group (Figure 3C).

The expression level of YAP was regulated using a plasmid vector or small interfering RNA (siRNA) *in vitro* and was correlated with the ligament-related gene expression levels. After transfection for 6 h and incubation for 48 h, the expression of YAP and type I collagen proteins was increased by a YAP plasmid vector compared to an empty plasmid vector in ACL-derived cells (Figure 4A). Overexpression of YAP showed a positive correlation with the mRNA expression of type I collagen and tenascin C ($p < 0.05$); however, there was no correlation in expression of type III collagen and actin alpha 2 (ACTA2) (Figure 4B). Five different YAP siRNAs were designed, and transfection was performed in ACL-derived cells that then were incubated for 24 h (Figure 4C). Underexpression of YAP showed a negative correlation with mRNA expression of type I collagen ($p < 0.05$); however, there was no significant correlation with the expression of type III collagen, tenascin C, or ACTA2 (Figure 4D).

Collagen fiber formation assessment

The diameter distribution of collagen fibrils serves as a crucial indicator in both healthy and damaged tissues. Therefore, a demonstration of matrix alignment in both groups was conducted using transmission electron microscopy (TEM) on day 14. In the TEM image, a notable increase was observed in the diameter of collagen fibers in the cross-section in the compression group (Figure 5A), and an enhanced distribution of the diameter was quantitatively verified (Figure 5B). Moreover, the average diameter of collagen fibers significantly increased on day 14 in the compression group compared to the non-compression group ($p < 0.001$) (Figure 5C).

DISCUSSION

In this study, given scaffold-induced compression, ACL-derived cells reseeded to the tendon graft demonstrated superior cell survival and integration and resulted in higher gene expression levels of YAP and type I collagen compared to non-compressed cell-allograft composites *in vitro*. The translocation of YAP into the nucleus was correlated with higher expression of type I collagen in the compression group to support the potential role of mechanotransduction in the ligamentization process.

Mechanical stress is one of the critical factors in the regulation of ligament and tendon remodeling. The effect of mechanical stress on cells primarily depends on the type, magnitude, and duration of mechanical stress.[25,34] Many studies have been published on the impact of mechanical stress on ACL cells. Kim SG et al. demonstrated that ACL cells increased expression of types I and III collagen mRNA after cyclic stretching.[35] Lee CY et al. studied the effects of estrogen and mechanical loading on gene expression of major ligament components (e.g., collagen type I, type III, and biglycan). That group demonstrated that cyclic mechanical loading alone increased the gene expression of collagen type I but did not affect collagen type III and biglycan.[36,37] Furthermore, Canseco JA et al. used a 1:1 co-culture system of bone marrow stem cells and tenocytes to investigate mechanical stimulation on cells. They demonstrated that mechanical stimulation promoted proliferation and synthesis of tendon-related genes (Col1A1, tenascin C, and TNMD) and bone-related genes (COL1A1, ALP, and OPN);[38] however, little is known about the effects of mechanical stress on tenocytes or reseeded cells within the tendon graft. Indeed, the mechanical microenvironment of cells is largely determined by their neighboring cells and surrounding ECM, signifying mutual dependence. Spalazzi JP

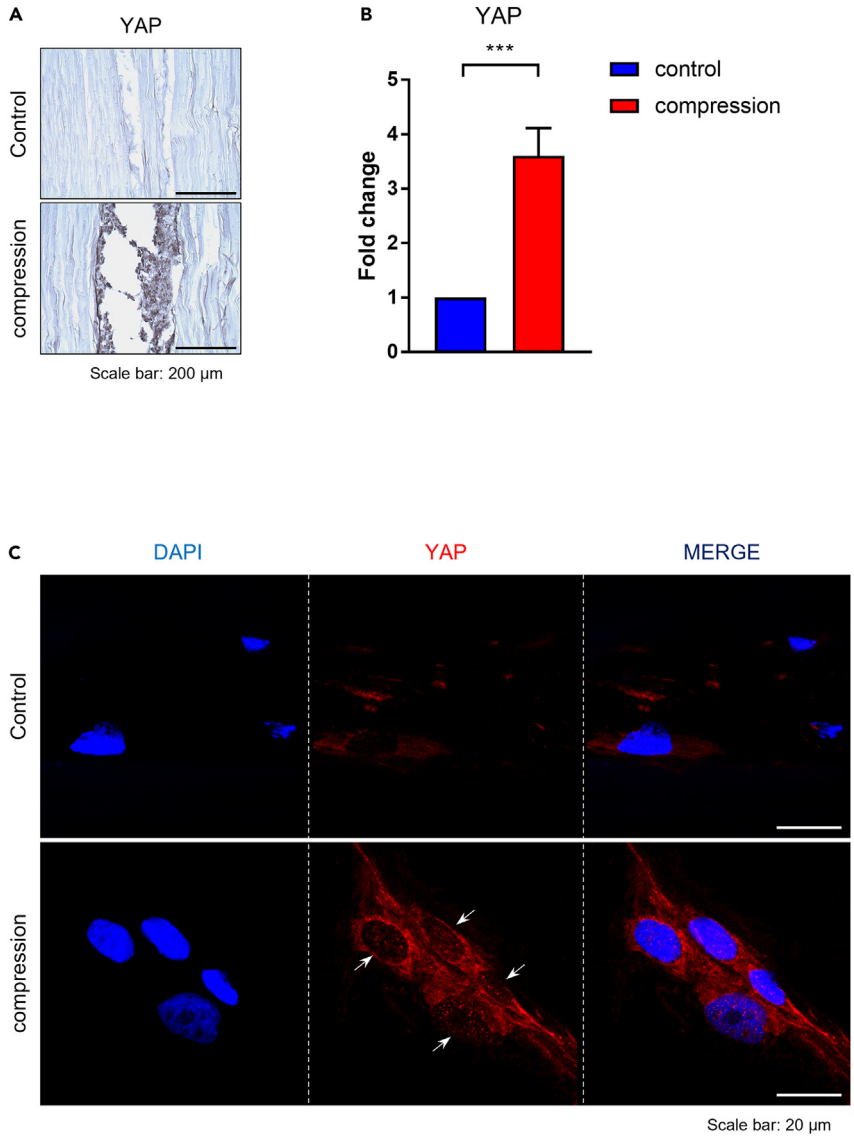

Figure 3. Expression of YAP by ACL-derived cells in tendon allograft

(A) YAP protein expression in the tendon allograft was confirmed by IHC staining on day 14. Magnification ×200, scale bar 100: μm.

(B) The mRNA expression of YAP was analyzed by RT-qPCR on day 14 (n = 3).

(C) Immunofluorescence staining was performed on day 14 for YAP (red). White arrow indicates that the YAP proteins translocated into the nucleus. *, $p < 0.05$; **, $p < 0.01$; ***, $p < 0.001$; ns: not significant. Statistical analysis of the data was performed using a two-tailed paired t-test. Data are shown as the mean ± SEM.

et al. applied scaffold-induced compression on tendon grafts and demonstrated upregulated expression of fibrocartilage-related markers and increased proteoglycan synthesis by tenocytes in the compressed tendon group.[34] Song F et al. studied the effect of mechanical loading created by continuous passive motion on tendon-bone healing in a rabbit ACLR model and demonstrated upregulated gene expression of type I collagen, alkaline phosphatase, osteopontin, tenascin C, and tenomodulin at the tendon-bone junction, in which the compressive load to the implanted graft is maximal.[39]

Our group has previously demonstrated that ACL-derived cells, when reseeded to the tendon graft, show an earlier ability to survive and integrate into tendon ECM, resulting in a higher gene expression level of type I collagen compared to adipose tissue-derived MSCs.[21] However, an additional tissue engineering strategy was required to enhance the survival and integration of ACL-derived cells in the ECM of the tendon graft. The FDA has approved a PCL-based nano scaffold of synthetic biodegradable aliphatic polymer that has a low melting temperature (60°C) and could be degraded through bulk erosion or hydrolysis. This nano scaffold has repeating hexanoate entities and could be utilized in clinical therapy because of its biocompatibility, stiffness, mechanical elasticity, biodegradability, non-toxicity, thermal stability,

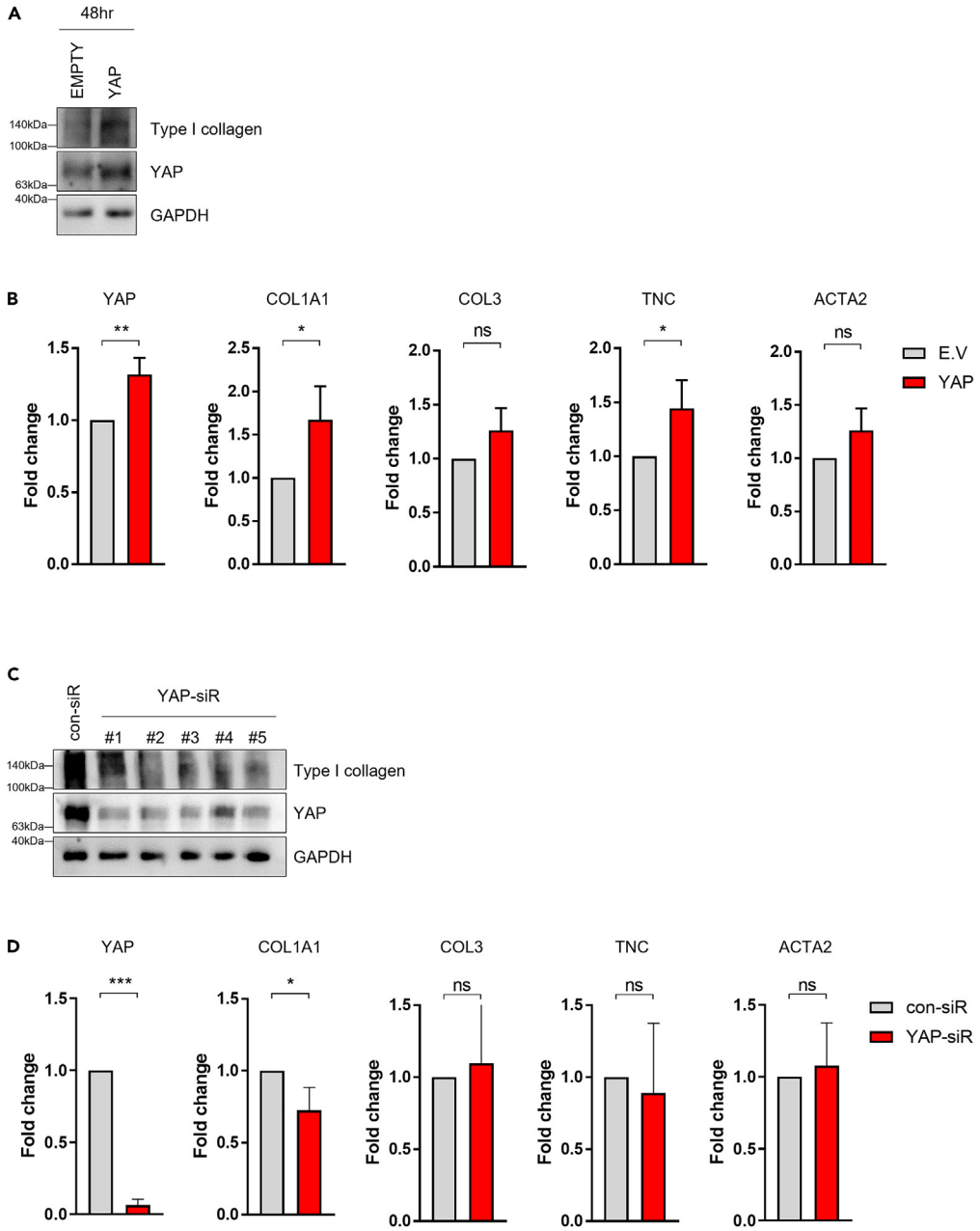

Figure 4. Expression of ligamentous factors by regulation of YAP in ACL-derived cells

(A) ACL-derived cells were transfected with YAP plasmid vector and incubated for 48 h, and YAP and type I collagen proteins were analyzed by immunoblotting.

(B) ACL-derived cells were transfected with YAP plasmid vector and incubated for 48 h, and the mRNA expression levels of YAP, COL1A1, COL3, TNC, and ACTA2 were analyzed by RT-qPCR (n = 3).

(C) ACL-derived cells were transfected with YAP siRNA and incubated for 24 h, and YAP and type I collagen proteins were analyzed by immunoblotting.

(D) ACL-derived cells were transfected with YAP plasmid vector and incubated for 24 h, and the mRNA expression levels of YAP, COL1A1, COL3, TNC, and ACTA2 were analyzed by RT-qPCR (n = 3). *, $p < 0.05$; **, $p < 0.01$; ***, $p < 0.001$; ns: not significant. Statistical analysis of the data was performed using a two-tailed paired t test. Data are shown as the mean ± SEM.

and rheological and viscoelastic properties.[40] These properties may allow future utilization in the actual clinical setting. Although the scaffold-induced compression was performed manually, the compression ratio was relatively uniform, reaching approximately 25%, which is in line with a previous study that applied a mechano-active nanofiber mesh scaffold on the tendon graft.[34]

YAP/TAZ are mechanotransducers that relay cytoskeletal tension to nuclei and regulate cellular biological outputs in response to mechanical cues. High ECM stiffness promotes cell spreading and leads to subsequent actin cytoskeleton tension, which promotes nuclear

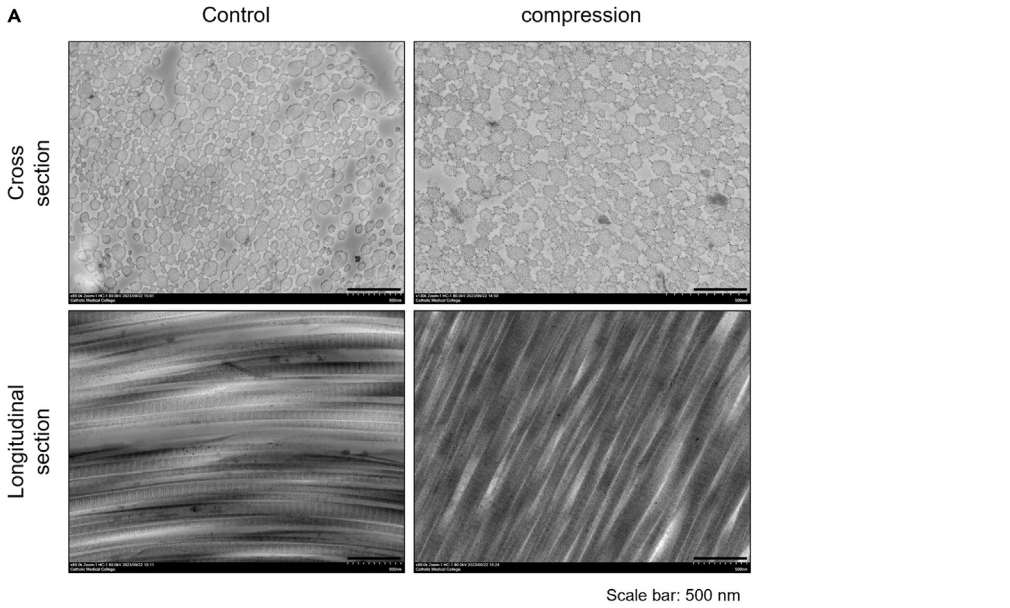

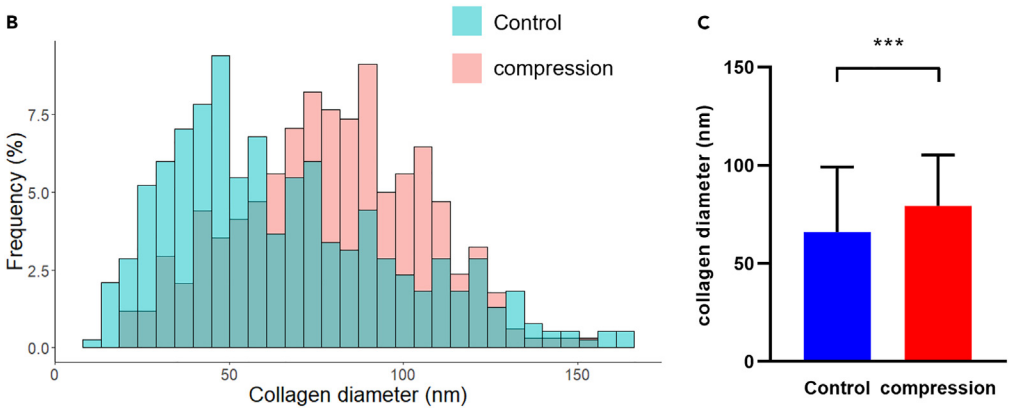

Figure 5. Measurement of collagen fibril diameter and alignment

(A) Cross and longitudinal section image of collagen fibrils obtained from the TEM in the tendon allograft on day 14. Magnification x 20,000, scale bar: 500 nm. In each groups, the diameter of collagen fibers was measured using ImageJ (n = 3), and the distribution (B) and mean values (C) of collagen fiber diameter were quantitatively presented. *, $p < 0.05$; **, $p < 0.01$; ***, $p < 0.001$; ns: not significant. Statistical analysis of the data was performed using a two-tailed paired t test. Data are shown as the mean ± SEM.

translocation of YAP/TAZ. The actin cytoskeleton has been reported to regulate YAP and TAZ via both Hippo-dependent and -independent pathways.[27] Compressive stress-induced mechanotransduction could cause the formation of F-actin through the aggregation of G-actin, and activated F-actin induces the translocation of YAP and TAZ through the Rho/ROCK signal pathway.[33,41,42] The exact mechanism of YAP/TAZ-regulated mechanotransduction needs further clarification in future studies.

In conclusion, given scaffold-induced compression, ACL-derived cells reseeded to the tendon graft demonstrated superior cell survival and integration. These cells produced higher gene expression level of type I collagen compared to non-compressed cell-allograft composites *in vitro*. Translocation of YAP into the nucleus was correlated with higher expression of type I collagen in the compression group to support the potential role of mechanotransduction in the ligamentization process.

Limitations of the study

This study has several limitations. First, scaffold-induced compression was performed manually, which may have affected the outcomes. However, the compression ratio measured using the ImageJ program was relatively uniform at approximately 25%. Second, only compressive

mechanical stress was evaluated in this study. Following the ACLR, the implanted tendon graft should encounter some degree of tensile and shear stresses combined.[43] The effects of various mechanical stresses on the tendon graft need to be assessed in future studies. Third, the study is limited by its nature as an *in vitro* study. As the experiment was performed without tensioning the graft, which would be possible in the *in vivo* study design, the alignment and diameter of collagen fibrils of the graft and the mechanical strengths of the final construct are unknown. Finally, mRNA gene expression levels were the primary outcomes, and the quantification of newly synthesized proteins remains unknown.

STAR★METHODS

Detailed methods are provided in the online version of this paper and include the following:

- KEY RESOURCES TABLE
- RESOURCE AVAILABILITY
  - Lead contact
  - Materials availability
  - Data and code availability
- EXPERIMENTAL MODEL AND STUDY PARTICIPANT DETAILS
  - Patients
- METHOD DETAILS
  - Isolation and culture of human ACL-derived cells
  - Experiment design
  - Histological analysis
  - Immunohistochemistry (IHC)
  - Immunofluorescence (IF)
  - RT-qPCR
  - Immunoblotting
  - Transmission electron microscopy (TEM)
- QUANTIFICATION AND STATISTICAL ANALYSIS

SUPPLEMENTAL INFORMATION

Supplemental information can be found online at https://doi.org/10.1016/j.isci.2023.108521.

ACKNOWLEDGMENTS

This work was supported by the National Research Foundation of Korea (grant number: 2020R1F1A1049719and 2021R1A6A1A03038899) and the Korean Fund for Regenerative Medicine(KFRM) grant funded by the Korea government (the Ministry of Science and ICT, the Ministry of Health & Welfare) (grant number: RS-2023-00215515).

AUTHOR CONTRIBUTIONS

J.P.: writing – original draft, formal analysis, investigation; H.S.: writing – original draft, data curation; S.J.: formal analysis, methodology, visualization; S.W.: investigation, formal analysis; S.L.: investigation; J.P.: investigation; M.L.: resources, methodology; T.K.: validation, funding acquisition; I.S.: conceptualization, resources; J.L.: writing – original draft, review, editing, validation, resources, funding acquisition, project administration.

DECLARATION OF INTERESTS

The authors declare no competing interests.

Received: June 15, 2023
Revised: November 13, 2023
Accepted: November 20, 2023
Published: November 23, 2023

REFERENCES

1. Duquin, T.R., Wind, W.M., Fineberg, M.S., Smolinski, R.J., and Buyea, C.M. (2009). Current trends in anterior cruciate ligament reconstruction. J. Knee Surg. *22*, 7–12.
2. Murray, M.M., Martin, S.D., Martin, T.L., and Spector, M. (2000). Histological changes in the human anterior cruciate ligament after rupture. J. Bone Joint Surg. Am. *82*, 1387–1397.
3. Lee, D.W., Shim, J.C., Yang, S.J., Cho, S.I., and Kim, J.G. (2019). Functional Effects of Single Semitendinosus Tendon Harvesting in Anatomic Anterior Cruciate Ligament Reconstruction: Comparison of Single versus

Dual Hamstring Harvesting. Clin. Orthop. Surg. *11*, 60–72.
4. Chung, K.S., Kim, J.H., Kong, D.H., Park, I., Kim, J.G., and Ha, J.K. (2022). An Increasing Trend in the Number of Anterior Cruciate Ligament Reconstruction in Korea: A Nationwide Epidemiologic Study. Clin. Orthop. Surg. *14*, 220–226.
5. Dallo, I., Chahla, J., Mitchell, J.J., Pascual-Garrido, C., Feagin, J.A., and LaPrade, R.F. (2017). Biologic Approaches for the Treatment of Partial Tears of the Anterior Cruciate Ligament: A Current Concepts Review. Orthop. J. Sports Med. *5*.
6. Juneja, S.C., and Veillette, C. (2013). Defects in tendon, ligament, and enthesis in response to genetic alterations in key proteoglycans and glycoproteins: a review. Arthritis *2013*, 154812.
7. Yao, S., Fu, B.S., and Yung, P.S. (2021). Graft healing after anterior cruciate ligament reconstruction (ACLR). Asia Pac. J. Sports Med. Arthrosc. Rehabil. Technol. *25*, 8–15.
8. Wang, H.D., Li, Z., Hu, X., and Ao, Y. (2022). Efficacy of Stem Cell Therapy for Tendon Graft Ligamentization After Anterior Cruciate Ligament Reconstruction: A Systematic Review. Orthop. J. Sports Med. *10*.
9. Lui, P.P., Wong, O.T., and Lee, Y.W. (2014). Application of tendon-derived stem cell sheet for the promotion of graft healing in anterior cruciate ligament reconstruction. Am. J. Sports Med. *42*, 681–689.
10. Lu, C.C., Ho, C.J., Huang, H.T., Lin, S.Y., Chou, S.H., Chou, P.H., Ho, M.L., and Tien, Y.C. (2021). Effect of Freshly Isolated Bone Marrow Mononuclear Cells and Cultured Bone Marrow Stromal Cells in Graft Cell Repopulation and Tendon-Bone Healing after Allograft Anterior Cruciate Ligament Reconstruction. Int. J. Mol. Sci. *22*.
11. Sun, Y., Chen, W., Hao, Y., Gu, X., Liu, X., Cai, J., Liu, S., Chen, J., and Chen, S. (2019). Stem Cell-Conditioned Medium Promotes Graft Remodeling of Midsubstance and Intratunnel Incorporation After Anterior Cruciate Ligament Reconstruction in a Rat Model. Am. J. Sports Med. *47*, 2327–2337.
12. Wei, X., Mao, Z., Hou, Y., Lin, L., Xue, T., Chen, L., Wang, H., and Yu, C. (2011). Local administration of TGFbeta-1/VEGF165 gene-transduced bone mesenchymal stem cells for Achilles allograft replacement of the anterior cruciate ligament in rabbits. Biochem. Biophys. Res. Commun. *406*, 204–210.
13. Amiel, D., Kleiner, J.B., Roux, R.D., Harwood, F.L., and Akeson, W.H. (1986). The phenomenon of "ligamentization": anterior cruciate ligament reconstruction with autogenous patellar tendon. J. Orthop. Res. *4*, 162–172.
14. Marieswaran, M., Jain, I., Garg, B., Sharma, V., and Kalyanasundaram, D. (2018). A Review on Biomechanics of Anterior Cruciate Ligament and Materials for Reconstruction. Appl. Bionics Biomech. 4657824.
15. Goradia, V.K., Rochat, M.C., Grana, W.A., Rohrer, M.D., and Prasad, H.S. (2000). Tendon-to-bone healing of a semitendinosus tendon autograft used for ACL reconstruction in a sheep model. Am. J. Knee Surg. *13*, 143–151.
16. Ng, G.Y., Oakes, B.W., Deacon, O.W., McLean, I.D., and Eyre, D.R. (1996). Long-term study of the biochemistry and biomechanics of anterior cruciate ligament-patellar tendon autografts in goats. J. Orthop. Res. *14*, 851–856.
17. Scheffler, S., Dustmann, M., Gangey, I., Schulz, T., Unterhauser, F., and Weiler, A. (2005). The biological healing and restoration of the mechanical properties of free soft-tissue allografts lag behind autologous ACL reconstruction in the sheep model. Trans. Orthop. Res. *51*, 0236.
18. Leong, N.L., Petrigliano, F.A., and McAllister, D.R. (2014). Current tissue engineering strategies in anterior cruciate ligament reconstruction. J. Biomed. Mater. Res. *102*, 1614–1624.
19. Nau, T., and Teuschl, A. (2015). Regeneration of the anterior cruciate ligament: Current strategies in tissue engineering. World J. Orthop. *6*, 127–136.
20. Petrigliano, F.A., McAllister, D.R., and Wu, B.M. (2006). Tissue engineering for anterior cruciate ligament reconstruction: a review of current strategies. Arthroscopy *22*, 441–451.
21. Park, J., Jo, S., Lee, M.K., Kim, T.H., Sung, I.H., and Lee, J.K. (2022). Comparison of ligamentization potential between anterior cruciate ligament-derived cells and adipose-derived mesenchymal stem cells reseeded to acellularized tendon allograft. Bone Joint Res. *11*, 777–786.
22. Docking, S., Samiric, T., Scase, E., Purdam, C., and Cook, J. (2013). Relationship between compressive loading and ECM changes in tendons. Muscles Ligaments Tendons J. *3*, 7–11.
23. Benjamin, M., and Ralphs, J.R. (1998). Fibrocartilage in tendons and ligaments–an adaptation to compressive load. J. Anat. *193*, 481–494.
24. Wren, T.A., Beaupre, G.S., and Carter, D.R. (2000). Mechanobiology of tendon adaptation to compressive loading through fibrocartilaginous metaplasia. J. Rehabil. Res. Dev. *37*, 135–143.
25. Killian, M.L., Cavinatto, L., Galatz, L.M., and Thomopoulos, S. (2012). The role of mechanobiology in tendon healing. J. Shoulder Elbow Surg. *21*, 228–237.
26. Cai, X., Wang, K.C., and Meng, Z. (2021). Mechanoregulation of YAP and TAZ in Cellular Homeostasis and Disease Progression. Front. Cell Dev. Biol. *9*, 673599.
27. Dupont, S., Morsut, L., Aragona, M., Enzo, E., Giulitti, S., Cordenonsi, M., Zanconato, F., Le Digabel, J., Forcato, M., Bicciato, S., et al. (2011). Role of YAP/TAZ in mechanotransduction. Nature *474*, 179–183.
28. Cobbaut, M., Karagil, S., Bruno, L., Diaz de la Loza, M.D.C., Mackenzie, F.E., Stolinski, M., and Elbediwy, A. (2020). Dysfunctional Mechanotransduction through the YAP/TAZ/Hippo Pathway as a Feature of Chronic Disease. Cells *9*.
29. Chu, G., Yuan, Z., Zhu, C., Zhou, P., Wang, H., Zhang, W., Cai, Y., Zhu, X., Yang, H., and Li, B. (2019). Substrate stiffness- and topography-dependent differentiation of annulus fibrosus-derived stem cells is regulated by Yes-associated protein. Acta Biomater. *92*, 254–264.
30. Scott, K.E., Fraley, S.I., and Rangamani, P. (2021). A spatial model of YAP/TAZ signaling reveals how stiffness, dimensionality, and shape contribute to emergent outcomes. Proc. Natl. Acad. Sci. USA *118*.
31. Hu, D., Jiang, J., Ding, B., Xue, K., Sun, X., and Qian, S. (2021). Mechanical Strain Regulates Myofibroblast Differentiation of Human Scleral Fibroblasts by YAP. Front. Physiol. *12*, 712509.
32. Komatsu, N., Kajiya, M., Motoike, S., Takewaki, M., Horikoshi, S., Iwata, T., Ouhara, K., Takeda, K., Matsuda, S., Fujita, T., and Kurihara, H. (2018). Type I collagen deposition via osteoinduction ameliorates YAP/TAZ activity in 3D floating culture clumps of mesenchymal stem cell/extracellular matrix complexes. Stem Cell Res. Ther. *9*, 342.
33. Ke, W., Wang, B., Hua, W., Song, Y., Lu, S., Luo, R., Li, G., Wang, K., Liao, Z., Xiang, Q., et al. (2021). The distinct roles of myosin IIA and IIB under compression stress in nucleus pulposus cells. Cell Prolif. *54*, e12987.
34. Spalazzi, J.P., Vyner, M.C., Jacobs, M.T., Moffat, K.L., and Lu, H.H. (2008). Mechanoactive scaffold induces tendon remodeling and expression of fibrocartilage markers. Clin. Orthop. Relat. Res. *466*, 1938–1948.
35. Kim, S.G., Akaike, T., Sasagaw, T., Atomi, Y., and Kurosawa, H. (2002). Gene expression of type I and type III collagen by mechanical stretch in anterior cruciate ligament cells. Cell Struct. Funct. *27*, 139–144.
36. Lee, C.Y., Liu, X., Smith, C.L., Zhang, X., Hsu, H.C., Wang, D.Y., and Luo, Z.P. (2004). The combined regulation of estrogen and cyclic tension on fibroblast biosynthesis derived from anterior cruciate ligament. Matrix Biol. *23*, 323–329.
37. Lee, C.Y., Smith, C.L., Zhang, X., Hsu, H.C., Wang, D.Y., and Luo, Z.P. (2004). Tensile forces attenuate estrogen-stimulated collagen synthesis in the ACL. Biochem. Biophys. Res. Commun. *317*, 1221–1225.
38. Canseco, J.A., Kojima, K., Penvose, A.R., Ross, J.D., Obokata, H., Gomoll, A.H., and Vacanti, C.A. (2012). Effect on ligament marker expression by direct-contact co-culture of mesenchymal stem cells and anterior cruciate ligament cells. Tissue Eng. Part A *18*, 2549–2558.
39. Song, F., Jiang, D., Wang, T., Wang, Y., Chen, F., Xu, G., Kang, Y., and Zhang, Y. (2017). Mechanical Loading Improves Tendon-Bone Healing in a Rabbit Anterior Cruciate Ligament Reconstruction Model by Promoting Proliferation and Matrix Formation of Mesenchymal Stem Cells and Tendon Cells. Cell. Physiol. Biochem. *41*, 875–889.
40. Chen, X., Chen, G., Wang, G., Zhu, P., and Gao, C. (2020). Recent progress on 3D-printed polylactic acid and its applications in bone repair. Adv. Eng. Mater. *22*, 1901065.
41. Guo, X., Wang, X., Tang, H., Ren, Y., Li, D., Yi, B., and Zhang, Y. (2022). Engineering a Mechanoactive Fibrous Substrate with Enhanced Efficiency in Regulating Stem Cell Tenodifferentiation. ACS Appl. Mater. Interfaces.
42. Boyle, S.T., Kular, J., Nobis, M., Ruszkiewicz, A., Timpson, P., and Samuel, M.S. (2020). Acute compressive stress activates RHO/ROCK-mediated cellular processes. Small GTPases *11*, 354–370.
43. Theopold, J., Schleifenbaum, S., Georgi, A., Schmidt, M., Henkelmann, R., Osterhoff, G., and Hepp, P. (2020). The single-suture technique for anterior cruciate ligament graft preparation provides similar stability as a three-suture technique: a biomechanical *in vitro* study in a porcine model. Arch. Orthop. Trauma Surg. *140*, 511–516.
44. Lee, J.K., Jo, S., Lee, Y.L., Park, H., Song, J.S., Sung, I.H., and Kim, T.H. (2020). Anterior cruciate ligament remnant cells have different potentials for cell differentiation based on their location. Sci. Rep. *10*, 3097.

45. Weiler, A., Forster, C., Hunt, P., Falk, R., Jung, T., Unterhauser, F.N., Bergmann, V., Schmidmaier, G., and Haas, N.P. (2004). The influence of locally applied platelet-derived growth factor-BB on free tendon graft remodeling after anterior cruciate ligament reconstruction. Am. J. Sports Med. *32*, 881–891.

46. Vangsness, C.T., Jr., Garcia, I.A., Mills, C.R., Kainer, M.A., Roberts, M.R., and Moore, T.M. (2003). Allograft transplantation in the knee: tissue regulation, procurement, processing, and sterilization. Am. J. Sports Med. *31*, 474–481.

47. Yu, Y.N., Ding, C., Cai, Z.N., and Chen, X.R. (1986). Cell cycle effects on the basal and DNA-damaging-agent-stimulated ADPRT activity in cultured mammalian cells. Mutat. Res. *174*, 233–239.

48. Jo, S., Wang, S.E., Lee, Y.L., Kang, S., Lee, B., Han, J., Sung, I.H., Park, Y.S., Bae, S.C., and Kim, T.H. (2018). IL-17A induces osteoblast differentiation by activating JAK2/STAT3 in ankylosing spondylitis. Arthritis Res. Ther. *20*, 115.

49. Beisbayeva, Z., Zhanbassynova, A., Kulzhanova, G., Mukasheva, F., and Erisken, C. (2021). Change in Collagen Fibril Diameter Distribution of Bovine Anterior Cruciate Ligament upon Injury Can Be Mimicked in a Nanostructured Scaffold. Molecules *26*.

50. Ruan, D., Zhu, T., Huang, J., Le, H., Hu, Y., Zheng, Z., Tang, C., Chen, Y., Ran, J., Chen, X., et al. (2019). Knitted Silk-Collagen Scaffold Incorporated with Ligament Stem/Progenitor Cells Sheet for Anterior Cruciate Ligament Reconstruction and Osteoarthritis Prevention. ACS Biomater. Sci. Eng. *5*, 5412–5421.

STAR★METHODS

KEY RESOURCES TABLE

REAGENT or RESOURCE	SOURCE	IDENTIFIER
Antibodies		
Rabbit anti-COL1A1 antibody	Santacruz	sc-8784
Rabbit anti-YAP antibody	ABclonal	A1002
Rat anti-Ki67 antibody	Invitrogen	14-5698-82
Rabbit anti-GAPDH antibody	Cell signaling	2118
Goat anti-Rat IgG (H + L) Cross-Adsorbed Secondary Antibody, Alexa Fluor™ 488	Invitrogen	A11006
Goat anti-Rabbit IgG (H + L) Cross-Adsorbed Secondary Antibody, Cyanine3	Invitrogen	A10520
Goat Anti-Rabbit IgG (H + L) Antibody, Biotinylated	Vector Lab	BA-1000
Biological samples		
Human tibialis tendon grafts	The Korea Public Tissue Bank	Korean
Oligonucleotides		
Primers for RT-qPCR, see Table S1	Macrogen	N/A
Software and algorithms		
ImageJ software	National Institute of Health	N/A
GraphPad Prism 7.0	GraphPad Software Dotmatics, Inc.	N/A

RESOURCE AVAILABILITY

Lead contact

Jin Kyu Lee (jklee77@hanyang.ac.kr).

Materials availability

Further information for resources and reagents generated in this study can be requested from the lead contact, Jin Kyu Lee.

Data and code availability

- All data reported in this paper will be shared by the lead contact, Jin Kyu Lee, upon request.
- This paper does not report original code.
- Any additional information required to re-analyse the data reported in this paper is available from the lead contact, Jin Kyu Lee, upon request.

EXPERIMENTAL MODEL AND STUDY PARTICIPANT DETAILS

Patients

The study was executed in agreement with institutional guidelines and approval from the Ethics Committee of Hanyang University Hospital. Written informed consent was obtained from all patients (IRB-2018-05-001). From January 2019 to December 2020, ruptured ACL remnant tissues were isolated from 8 patients (5 males and 3 females) with an average age of 21.9 $\pm$ 3.2 years (range, 20–29 years) who underwent primary ACLR within 4 weeks of injury.

METHOD DETAILS

Isolation and culture of human ACL-derived cells

The experimental protocol for ACL-derived cell isolation was previously described by Lee et al.[44] Briefly, obtained ACL remnant tissues were cut into small < 1cm segments using scissors. The tissue segments were washed twice using 1x PBS and enzymatically dissolved with 1 mg/mL of collagenase type I (Gibco, 17100-017; sigma, C0130) in serum-free DMEM containing penicillin-streptomycin (Thermo Fisher, 15140122).

Cell suspensions were filtered using a 70-μm cell strainer (SPL, 93070), and cells were isolated after centrifugation at 1400 rpm for 3 min. Isolated ACL-derived cells were stored in a deep freezer at −80°C. All experiments were performed using third passage ACL-derived cells.

Experiment design

A total of 8 strips of donated human acellularized tibialis tendon allografts was obtained from the Korea Public Tissue Bank. All tendon allografts were decellularized and sterilized through the standard protocols.[45–47] Briefly, the tendon allografts were cut to a length of 1.5 cm before injection of cells. Cells suspensions (150 μL) containing 1 x 10^6 ACL-derived cells were prepared for reseeding. Each tendon segment was reseeded with ACL-derived cells by injecting directly into the graft using a 25-gauge needle. The injection was performed into the core of the graft and monitored for any leakages.[21] The nanofiber PCL scaffold (Artipore Bilaminate, ST-1) was cut into a rectangular shape with a length of 3 cm and a width of 1 cm. After injection of cell suspensions containing ACL-derived cells into the tendon allograft, the cell-tendon graft composites were manually compressed with a nanofiber PCL scaffold at the middle and sealed with Tissel (Baxter), a sealant solution (Figure S1). The cell-tendon graft composites were placed in DMEM growth media containing 10% fetal bovine serum (FBS) and 1% penicillin-streptomycin and incubated in a 5% CO_2 incubator at 37°C for one, seven, or 14 days. The compression ratio of each cell-tendon graft composite was measured. The frozen tissue blocks were cryo-sectioned longitudinally at 6-μm thickness, and the most representative slide with the broadest tissue diameter was chosen with the agreement of three assessors. The ImageJ software (National Institutes of Health, Bethesda, MD, USA) (n = 8) was used for measurements. In the image, a vertical line was drawn parallel to the side of the tissue or the scaffold. Diameters were measured perpendicularly between vertical lines at the graft's distal, middle, and proximal aspects for comparison (Figure S2). A single assessor (JSP) repeated all measurements three times. A mean value was adopted for calculations.

Histological analysis

Cryo-sectioned slides at 6-μm thickness were used for histological analysis. The staining procedures were conducted following the standard protocols indicated in the manufacturer's instructions. Hematoxylin and eosin (H&E) stain was used for histologic and cytologic analyses, and Picrosirius red (PSR; Abcam, ab150681) was used for types I and III collagen analysis. All stained slides were mounted using a permanent mounting medium (Vector Labs, H-5000). Images of cells injected into the tendon allografts were observed at 200x magnification using bright-field microscopy, and the number of cells was counted on five consecutive slides. All measurements were analyzed by two independent observers blinded to each other.

Immunohistochemistry (IHC)

Immunohistochemical staining was performed following the protocols indicated in a previous study by Jo et al.[48] Briefly, the tissue slides were fixed with 100% cold acetone for 10 min and washed with flowing water for 10 min to remove the OCT compound (SAKURA, 4583). After washing with 1x PBS three times, tissue slides were incubated with 1x PBS including 0.3% Triton X-100 for 10 min and blocked with BLOXALL (Vector Lab, SP-6000) for 30 min at room temperature. The tissue slides were immunostained with primary antibody (COL1A1, Santa, 8784; 1:100 or YAP, ABclonal, A1002; 1:200) diluted with antibody diluent (DAKO, S3022) at room temperature for 1 h. After washing three times with 1x PBST, the tissue slides were incubated with biotinylated anti-rabbit IgG secondary antibodies (Vector Lab, BA-1000; 1:200) mixed with one drop of normal horse serum (Vector Lab, S-2012) for 1h. Consecutively, tissue slides were incubated with an ABC kit (Vector Lab, PK-6102) for 30 min and stained with a DAB substrate kit (Vector Lab, sk4100) for 1–5 min. Afterward, tissue slides were stained with hematoxylin (Merck, 1.05174.0500) for 10 s and dehydrated with gradually increasing ratios of ethanol solution (50–100% ethanol). Finally, tissue slides were mounted with a permanent mounting medium (Vector Lab, H-5000). Images were gathered with a Nikon Eclipse Ti-U microscope.

Immunofluorescence (IF)

The tissue slides were fixed in 100% cold acetone for 10 min and washed with flowing water to remove the OCT compound (SAKURA, 4583) for 10 min. After washing with 1x PBS three times, tissue slides were incubated with 1x PBS including 0.3% Triton X-100 for 10 min and blocked with BLOXALL (Vector Lab, SP-6000) for 30 min at room temperature. The tissue slides were immunostained with primary antibody (1:100) diluted with antibody diluent (DAKO, S3022) at 4°C overnight. After incubation and washing three times with 1x PBST, the slides were incubated with Alexa 488 or Cy3-conjugation secondary antibodies (1:100) diluted with antibody diluent for 1 h at room temperature. After incubation and washing three times with 1x PBST, tissue slides were mounted with mounting medium containing DAPI (Vector CA, USA). Images were obtained with a confocal microscope (Leica Microsystems). The primary antibodies used were: Ki-67 (Invitrogen, 14-5698-82), type I collagen (Santa, sc-8784), or YAP (ABclonal, A1002).

RT-qPCR

The tissue slides were scraped with a cell scraper and collected for mRNA analysis. RNA extraction was conducted following conventional methods with TRI-reagent; 1μg RNA for complementary DNA (cDNA) was used for reverse transcription PCR (RT-PCR). cDNA was used as the template for RT-qPCR. Primers for RT-qPCR were in Table S1.

Immunoblotting

Total protein extraction was performed following the conventional methods with 1x RIPA buffer containing phosphatase inhibitor (Cell Signaling, 5870S) and protease inhibitor (Calbiochem, 535140) on ACL-derived cells. Quantification of extracted proteins was conducted with a Bradford assay. A mount of 30 μg proteins was subjected to immunoblotting. The primary antibodies were GAPDH (Cell signaling, 2118), type I collagen (Santa, sc-8784), and YAP (ABclonal, A1002).

Transmission electron microscopy (TEM)

In the process of preparing for transmission electron microscopy (HT7800, Hitachi, japan) observation, the harvested tissues were fixed in a 2.5% glutaraldehyde solution at 4°C. Subsequently, to analysis by TEM, the process of samples was carried out following established methods.[49,50] The cross and longutidunal section were performed with an ultramicrotome (EM UC7, Leica Microsystems, German) to a thickness of 100 nm. In each sample, approximately 1000 collagen fibrils were selected through electron microscopy observation to measure the mean diameter and distribution of collagen fibrils between two groups. The ImageJ software (n = 3) was used for measurements.

QUANTIFICATION AND STATISTICAL ANALYSIS

All quantitative and statistical values of graph data were analyzed with Graph-Pad Prism 7.0. As appropriate, a two-tailed paired t-test or a two-way ANOVA was used for determination of statistical significance. The values are expressed as the mean ± standard error of the mean (SEM) obtained from at least three independent experiments.